Supporting Information for

Galectin-1-based Tumor-Targeting for Gold Nanostructure Mediated Photothermal Therapy

Samir V. Jenkins,[1] Dmitry A. Nedosekin,[2] Emily K. Miller,[3] Vladimir P. Zharov,[2] Ruud P.M. Dings,[1] Jingyi Chen,[3] Robert J. Griffin,[1]

[1]Department of Radiation Oncology and [2] Otolaryngology and Phillips Classic Laser and Nanomedicine Laboratories, University of Arkansas for Medical Sciences, Little Rock, AR, 72205 USA

[3]Department of Chemistry and Biochemistry, University of Arkansas, Fayetteville, AR, 72701, USA

Corresponding Author: Robert J. Griffin, 4301 W. Markham, Mail Slot #771, Little Rock, AR 72205. Email: rjgriffin@uams.edu

Keywords: Breast Cancer, Photoacoustic Microscopy, Photothermal, Gold Nanocage, Targeted Nanomedicine

Conflict of Interest: The authors declare no conflicts of interest.

Synthesis of Au nanocages (AuNCs).

The AuNCs were synthesized by galvanic replacement reaction between Ag nanocubes and $HAuCl_4$ as previously described.(1) First, Ag nanocubes were synthesized by the polyol method.(2) Briefly, 50 mL EG was added to a 250-mL round-bottom flask equipped with a stirring bar and placed in an oil bath at 150 ºC. After the temperature equilibrated (30~45 min), EG solutions of 0.6 mL of 3 mM NaHS, 5 mL of 3 mM HCl, 12.5 mL of PVP (0.25 g), and 4 mL of 282 mM AgTFA were sequentially added to the reaction flask. Once the LSPR peak reached ~440 nm (~35 min after addition of AgTFA), the reaction was quenched in an ice bath. Upon cooling, the product was collected by adding acetone to the reaction solution at a ratio of 5:1 and centrifuging at 6,000 rcf for 10 min. The resulting pellet was purified twice with H_2O and collected by centrifugation at 20,000 rcf for 10 min, and resuspended in 10 mL of H_2O for future use. To synthesize AuNCs, 10 mL of H_2O was heated to boiling in a 50-mL round-bottom flask equipped with a stirring bar. To the boiling liquid, 1 mL of the Ag nanocubes described above was added and subsequently 1 mM $HAuCl_4$ was added using a syringe pump at a rate of 45 mL/h until the LSPR maximum was at 750 nm. The AuNCs were purified by saturated NaCl solution to remove by-product AgCl, washed 3 times by centrifugation at 20,000 rcf for 10 min, and resuspended in H_2O at a concentration of 5 nM for future use.

Synthesis of PDA coated AuNCs (AuNC@PDA).

The AuNC@PDA were prepared by self polymerization of dopamine on the surface of AuNCs under basic conditions in the presence of O_2.(3) Briefly, 3 mL of 5 nM AuNC aqueous suspension was diluted to 200 mL using Tris-buffered saline (20 mM Tris and 100 mM NaCl, pH = 9) in a 250-mL, 3-neck, round-bottom flask. The reaction flask was briefly flushed with O_2 and placed in a bath sonicator held at 4 ºC with ice. Dopamine hydrochloride (0.2 mmol, 36.0 mg) was added to the flask, the vessel was sealed under 1 atm O_2, and the mixture was sonicated

throughout the reaction until the LSPR had redshifted ~50 nm (~75 min). After this reaction, the product was collected by centrifugation at 6,000 rcf for 10 min, washed with H_2O twice and recovered by centrifugation at 19,000 rcf for 10 min at 4 ºC. The AuNC@PDA was resuspended in H_2O at a concentration of 6 nM for characterization and future use.

Cell lines.

Murine breast cancer cells (4T1, ATCC CRL-2539) and murine endothelial cells (2H11, ATCC CRL-2163) were purchased and cultured in DMEM supplemented with 10% FBS and 1% P/S and passaged biweekly.

Photoacoustic Imaging

PA imaging and quantification of nanoparticles was performed using a custom laser scanning PA microscope coupled to inverted Olympus IX81 microscope (Olympus Inc., Center Valley, PA). Excitation laser (532 nm) was focused by a microscope objective (UPlanFl 10x or 100x for low resolution and high resolution imaging, respectively) from the bottom of the sample. A pair of galvo mirrors (6215H, Cambridge Technologies, Lexington, MA) steered laser beam across the sample in a XY raster pattern. The laser operated at 10 kHz pulse repetition rate. Acoustic waves were acquired using ultrasound transducers placed directly over the sample. The field of view was limited to 120 μm and 1.2 mm by the focal area of the transducers used for focused (20 MHz, V316, 12 mm focal distance, Olympus-NDT Inc,) and unfocused (3.5 MHz, model 6528101, 4.5 mm in diameter; Imasonic Inc., Besançon, France) transducers, respectively. The 35 mm dishes with cells were filled with 1X PBS to provide acoustic coupling with a transducer. Signals from transducer were amplified (5662B, Panametrics) and recorded by PC equipped with a high-speed digitizer (PCI-5124, 12-bit card, 128 MB of memory, National Instruments, Austin, TX). Control over the mirrors and overall synchronization of the system was performed using a digital waveform generator (DG4062, Rigol, Beijun, China). Wide area

imaging was performed using 3.5 MHz transducer in a mosaic mode by shifting sample position using a mechanical stage (ProScan II, Prior Scientific, Cambridge, UK) in 1.0 mm steps. All the individual PA images were stitched together in automated mode by a custom LabView based software.

Photoacoustic-Fluorescence Flow Cytometry.

The PAFFC system was described elsewhere.(4) Briefly, it was constructed in-house and based on a microscope platform (Nikon Eclipse E400, Nikon instruments, Inc., Melville, NY, USA), featuring an acoustic transducer (model 6528101, 3.5 MHz, 4.5 mm in diameter; Imasonic Inc., Besançon, France) mounted over flow cell on a XYZ positioning stage. The flow module (quartz capillary, Molex Inc., Phoenix, AZ) had a 100 μm square cross-section. Laser irradiation was delivered and fluorescence was collected by a 20× objective (PlanFluor, Nikon Instruments, Inc.). The setup was equipped with 820-nm diode-pumped pulsed laser (PA detection) maximal energy in the sample of 5 μJ; pulse duration, 8 ns; and pulse rate of 10 kHz (LUCE 820, Bright Solutions, Italy). Fluorescence was excited by 488 nm laser (IQ1C45 (488-60) G26, Power Tech., Alexander, AR, USA) having 7 mW power in the sample. Laser beams formed 5×150 μm lines in the capillary. PA signals from the transducer were amplified (preamplifier 5678; bandwidth, 200 kHz – 40 MHz; gain 40 dB; Panametrics NDT) and digitized (PCI-5124, 12-bit, 200 MSPS, National Instruments Inc.). Custom developed Labview software recorded PA/fluorescence signals. Transient fluorescence signals were used to identify individual cells in flow. For each cell the corresponding PA signal was calculated from PA data trace. Signal threshold set using control samples (no incubation with NPs) was used to identify cells containing NPs. All the data acquisition and analysis were performed using custom LabView based software.

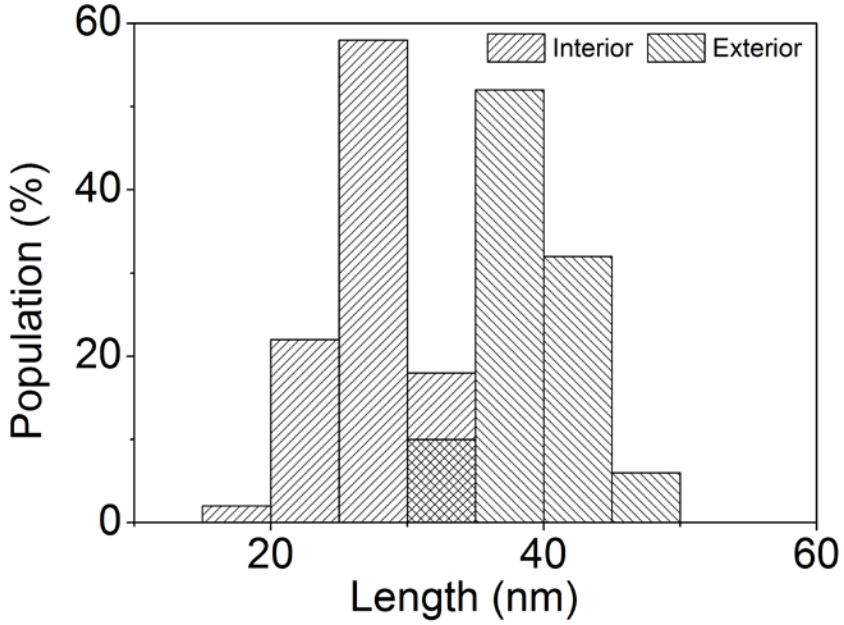

Figure S1. Measurement of interior and exterior edge lengths of AuNC as measured by TEM.

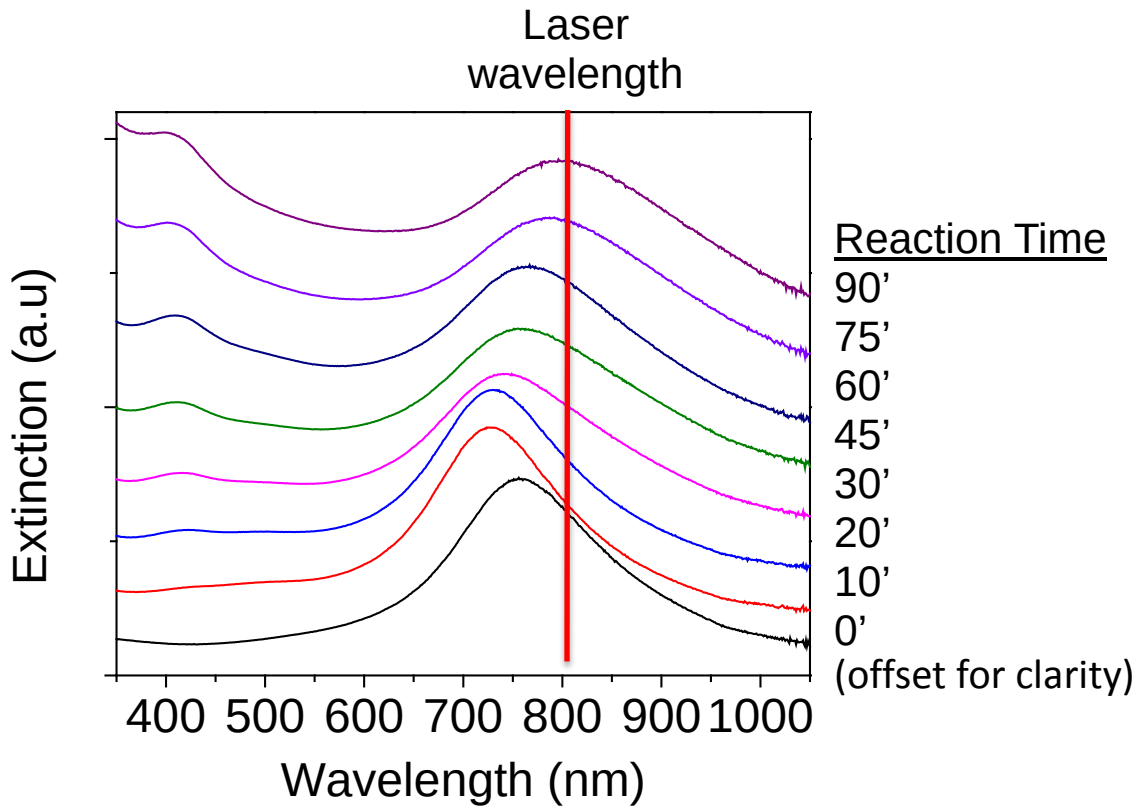

Figure S2 Extinction spectra of the reaction mixture during dopamine autopolymerization.

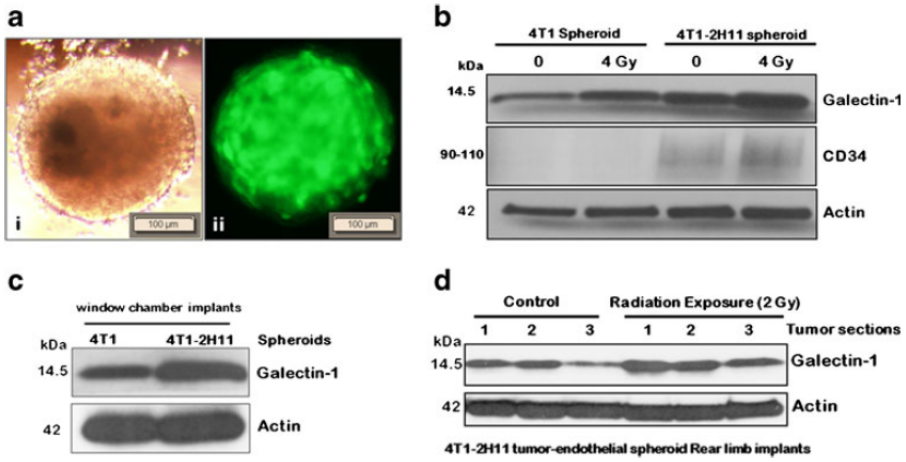

Fig. 6 Growth of tumor from tumor spheroids in dorsal skinfold window chamber implants and galectin-1 expression on radiation exposure. **a** (*i*) Phase contrast and (*ii*) fluorescence images of 7-day GFP-4T1-2H11 tumor-endothelial cell spheroid grown in a hanging drop of medium. **b** Elevated galectin-1 expression in 4T1-2H11 tumor-endothelial cell spheroids when compared to 4T1 tumor cell spheroids alone which is further induced in response to radiation exposure. CD34 is the tumor-endothelial cell marker and actin serves as the loading control. **c** Galectin-1 expression in lysates from tumors originating from spheroids in dorsal skinfold window chamber implants of nude mice. **d** Induction of galectin-1 expression in sections from tumors originating from tumor-endothelial cell spheroids in rear limb of nude mice upon radiation exposure of 2 Gy

Figure S3 Western blot of Galectin-1 expression in 4T1 and 2H11 cell spheroids normalized to Actin (from Upreti, 2013 (5))

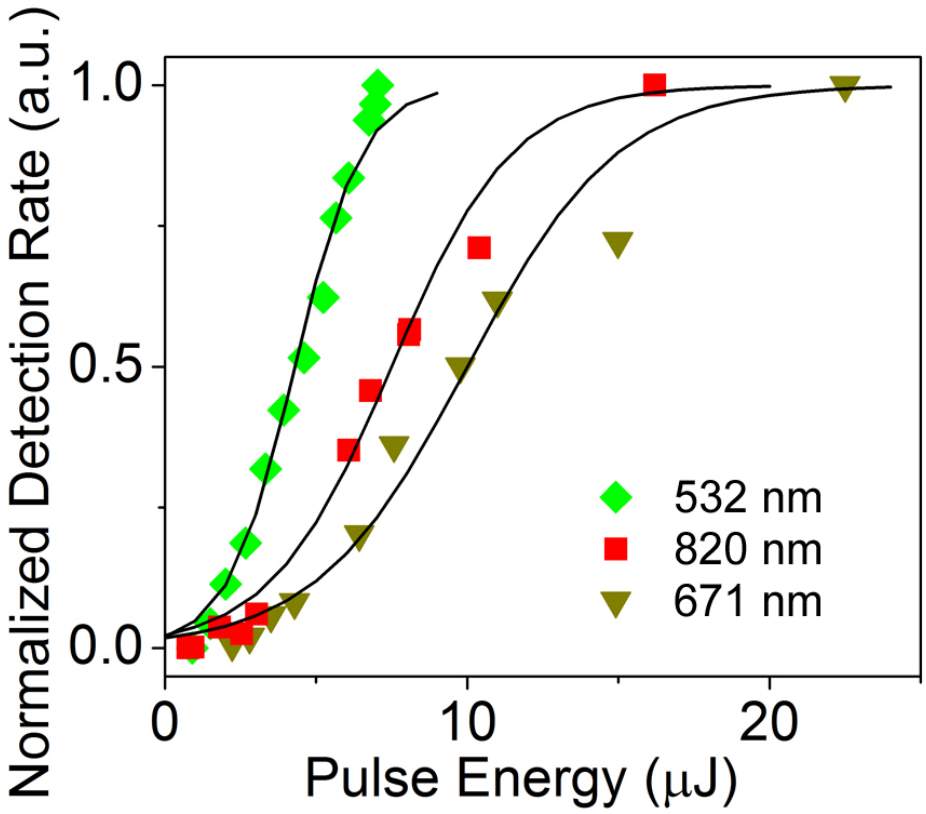

Figure S4 Normalized particle detection as a function of laser energy for 532 nm (diamonds), 671 nm (triangles), and 820 nm (squares) lasers. Black lines represent fitted lines.

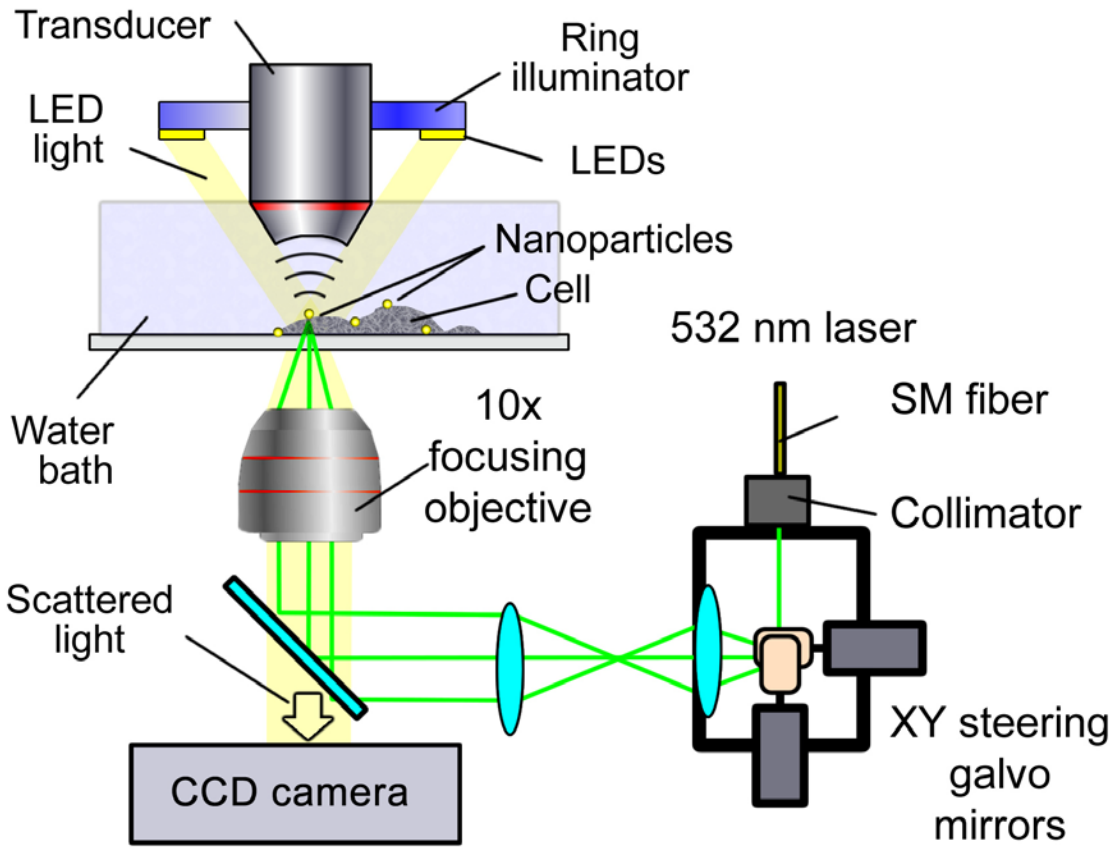

Figure S5 Schematic illustration of the photoacoustic microscopy system.

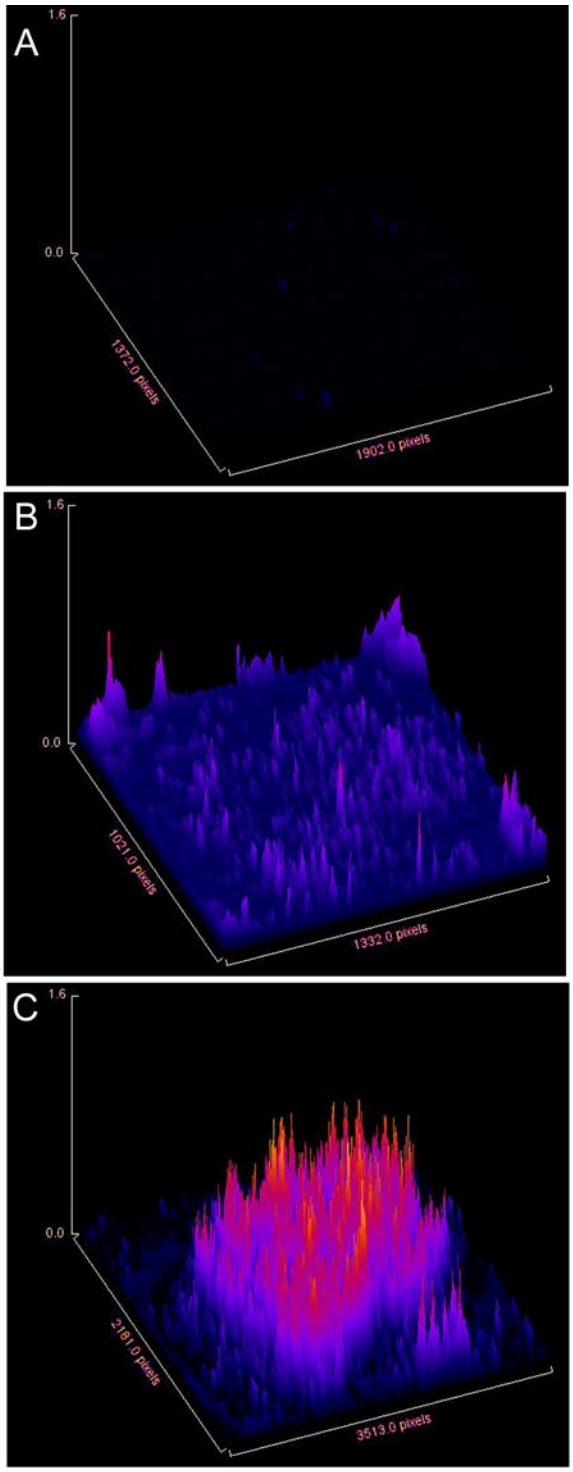

Figure S6. Photoacoustic mapping of ex vivo tumor tissue. Surface plot showing PA intensity at each pixel for 4T1 tumors treated with (A) AuNC@PDA, (B) AuNC@PDA-Ax (600 Ax/AuNC) and (C) AuNC@PDA-Ax (60,000 Ax/AuNC).

References

1. Skrabalak SE, Au L, Li X, Xia Y. Facile synthesis of Ag nanocubes and Au nanocages. Nat Protoc. 2007;2(9):2182-90.
2. Zhang Q, Li W, Wen L-P, Chen J, Xia Y. Facile Synthesis of Ag Nanocubes of 30 to 70 nm in Edge Length with CF(3)COOAg as a Precursor. Chemistry (Weinheim an der Bergstrasse, Germany). 2010;16(33):10234-9.
3. Meeker DG, Jenkins SV, Miller EK, Beenken KE, Loughran AJ, Powless A, et al. Synergistic Photothermal and Antibiotic Killing of Biofilm-Associated Staphylococcus aureus Using Targeted Antibiotic-Loaded Gold Nanoconstructs. ACS Infectious Diseases. 2016;2(4):241-50.
4. Nedosekin DA, Sarimollaoglu M, Foster S, Galanzha EI, Zharov VP, editors. Photoacoustic-fluorescence in vitro flow cytometry for quantification of absorption, scattering and fluorescence properties of the cells2013.
5. Upreti M, Jamshidi-Parsian A, Apana S, Berridge M, Fologea DA, Koonce NA, et al. Radiation-induced galectin-1 by endothelial cells: a promising molecular target for preferential drug delivery to the tumor vasculature. J Mol Med (Berl). 2013;91(4):497-506.